e-Polymers **2010**, no. 138 http://www.e-polymers.org
ISSN 1618-7229

A study on hybrid oligomeric type II photoinitiator

Guodong Ye,[1 2] Wenbo Kan,[2] Jianwen Yang,[2] Zhaohua Zeng,[2] Xiaoxuan Liu[3]*

[1]Department of Chemistry, Guangzhou Medical College, Guangzhou 510182, P. R. China.
[2*]School of Chemistry & Chemical Engineering, Sun Yat-Sen University, Guangzhou 510275, P. R. China; e-mail: ygdcn@163.com
[3]Department of Polymeric Material and Engineering, College of Material and Energy, Guangdong University of Technology, Guangzhou 510006, P. R. China.

(Received: 08 September, 2008; published: 01 December, 2010)

Abstract: Preparing tailor-made hybrid photoinitiator (PI) for specific applications continues to gain momentum. The hybrid PIs comprising both H-abstraction chromophore and coinitiator moiety are the candidate materials with energy-saving and environment-protection in the photo-curing field. So two oligomeric photoinitiators (OMKs) containing benzophenone (BP) and aliphatic *tert*-amines chromophore in the main-chain (OMK-2) or side-chain (OMK-1) were synthesized and characterized respectively. Photophysical investigation showed that the absorption maxima of OMKs were around 340 nm, red shifted about 5-10 nm compared to BP. Their initiation efficiencies were found to be higher than that of BP and 4,4'-bis(dimethylamino)benzophenone(MK) respectively. The reaction proceeds via a simple electron-transfer/proton-transfer mechanism. Dynamic NMR data reveal that H-abstraction reacts predominantly via alpha H of aliphatic *tert*-amines, as might be expected on the basis of the lower ionization potential and bond dissociation energy of aliphatic amines compared to aromatic amines. The reaction mechanism of H-abstraction was confirmed by using radical scavenger 2,2,6,6-tetramethylpiperidin-1-oxy(TEMPO), which acts as a probe under photolysis reaction conditions. The volatility and migration were tested under simulated conditions, the result show that OMKs exhibited very low volatility and significantly reduced migration compared to the low molecular analogs. Results showed that the OMKs are the promising candidate as higher efficient PIs with low volatile organic compounds (VOCs) emission and reduced migration. They are suitable for environmental-friendly formulations.

Introduction

Photoinitiators(PIs) are vital for photo-curing, they initiate photopolymerization of vinyl monomer. Usually they are divided into two classes: free radical and cationic. The former can be further divided into two types: cleavage (Type I) and H-abstraction (Type II).

In the last few years, preparing tailor-made hybrid PI for specific applications continues to gain momentum. The PIs bonded with thermal initiators, e.g. benzoin & azo-bis-isobutyronitrile, are used in the initial-light and post-heat dual-curing model system [1]. The free radical PIs incorporated with cationic PIs have been utilized to improve photo-curing wavelength selectivity of epoxy resin [2]. The cleavage PIs in conjunction with H-abstraction PIs, e.g. aminoalkylphenone & thioxanthone, have been applied to formulations based on TiO_2 [3].

The H-abstraction PIs linked with coinitiators(e.g. amine/alcohol) are one of the early hybrid PIs [4]. Some PIs are shown in Fig.1. They are expected to be the candidate materials with energy-saving and environment-protection in the photo-curing field. Whilst much effort has been directed towards the synthesis and characterization of the hybrid PIs, the works invariably cause problems. The main disadvantage is that the new compounds own low photoinitiated activity because of the obvious ‘‘back electron transfer’’ effect [5]. A typical example is MK, which possesses both BP chromophore and aromatic *tert*-amine group in its structure. Due to its relatively low efficiency, in most cases it is used in conjunction with BP and serves as a hydrogen donor, not as an efficient PI [6]. Clearly, there is still a need to optimize the molecular design of hybrid PIs for obtaining the desired performances.

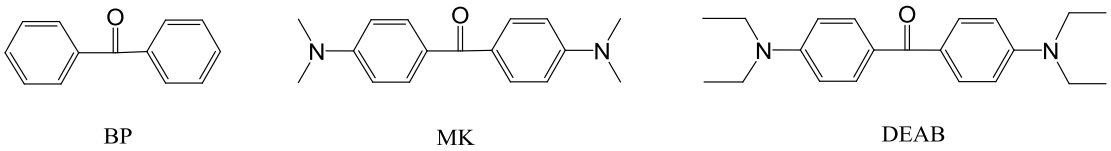

BP MK DEAB

Fig. 1. Structures of some type II PIs.

Recently, we have reported a hybrid PI containing amine-linked thioxanthones [7], an oligomeric PI containing aminoalkylphenone [8] , and a bifunctional PI bearing hydroxyalkylphenone structure [9]. As part of our continuing interest in novel photoinitiating systems, in this context, we report the synthesis and characterization of oligomeric OMKs. The high efficient OMKs were prepared by polycondensation, thus the molecular weight of OMKs could be adjusted more easily through this facile method than free radical polymerization. Certainly OMKs are expected to give low VOCs and migration because of the peculiarity of the polymeric systems

Results and discussion

Spectroscopic properties

-UV

The absorbance characteristics of different PIs are shown in Fig. 2 and the corresponding molar extinction coefficients (ε_{max}) are listed in Table 1.

OMKs have similar spectra which are typical for MK chromophore, i.e. absorbing strongly in far UV and possessing an absorption maximum of n-π* transitions (340nm) probably contained of charge transfer (CT) character (304nm). They also involve a weak π-π* transition centered at 242 nm. However, R. Liska believed the strong absorption at approx 340 nm in MK type PIs results from a shift of 252 nm absorption of BP (both π-π*). In the case of MK like PIs, the n-π* transition is overlaid by the π-π* transition. In addition, something worth mentioning here is that the n-π* transition has usually significantly lower extinction coefficient than π-π* due to the spin-forbidden transition. The different assignment will be discussed elsewhere. As the solvent polarity increases from cyclohexane to water, the UV/Vis absorption spectra of OMK show a significant hypsochromic shift of the long-wavelength band and a significant bathochromic shift of the short-wavelength band. Based on the results reported so far on such kinds of MK systems, it has been corroborated that the n-π* involves a transition from a polar ground state to an excited state with a lower dipole

moment. Thus, compared to gas phase the excited state is less solvated than the ground state, and this leads to an increase of the transition energy and hence a blue shift. The π-π* transition does not give any appreciable change in the dipole moment, but an increase in the dipole polarizability of the excited state leads to a larger solvation for the excited state and a decrease in the transition energy, a red shift. [10]

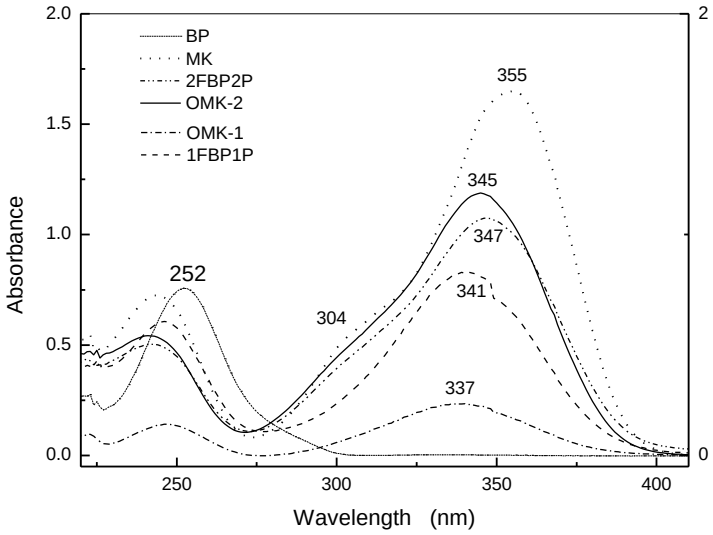

Fig. 2. The UV spectra of PIs in CH_2Cl_2.

Tab. 1. The UV/vis spectral characteristics of PIs.

Compound	λ(nm)	$\varepsilon(M^{-1}.cm^{-1})$	λ(nm)	$\varepsilon(M^{-1}.cm^{-1})$
BP	252	1.7×10^4	335	1.4×10^2
MK	244	1.7×10^4	355	3.8×10^4
2FBP2P	242	1.2×10^4	347	2.5×10^4
OMK-2	242	1.3×10^4	345	2.7×10^4
1FBP1P	246	6.2×10^3	341	8.5×10^3
OMK-1	246	9.6×10^3	337	2.0×10^4

More strikingly, n-π* transition of OMKs showed a strong and very broad peak centered at 347 nm and with a shoulder at around 304 nm. The preliminary results of quantum calculation reveal that the weak and very broad band of BP around 335 nm is composed by four transitions [11]. Considering this evidence, it seems that the broad band of OMK seen in the experiments is also a composite band caused by several transitions. It is likely that the natural broadening arises from the disordered structure of the solution or charge transfer (CT) transitions.

It was also found that the absorption maxima of four PIs containing MK chromophore were above 335 nm, red shifted about 2-10 nm compared to BP. This is mainly due to substitution of a piperazine ring group (electron-donating group) at the *para*-

position to the aromatic ring of the BP group. The absorption character well matches the emission profile of the industrial mercury lamp used in UV coating technology, and thus benefits the photoinitiation efficiency.

The similarity of UV/vis. spectra of OMKs to that of MK indicates that they possess an excitation process similar to MK during irradiation. Moreover, it indicates that the TEGDA/TMPTA residue has no significant influence on the UV/vis absorption shape of MK moieties in OMK. High extinction coefficient (~10^4) ensures a considerable absorption of the incident light at a relatively low concentration of the PI in the polymer matrix.

-Fluorescence

The steady state fluorescence spectra of PIs including OMK-1, OMK-2 and their corresponding intermediate (1FBP1P, 2FBP2P) as well as MK in CH_2Cl_2 are shown in Fig. 3.

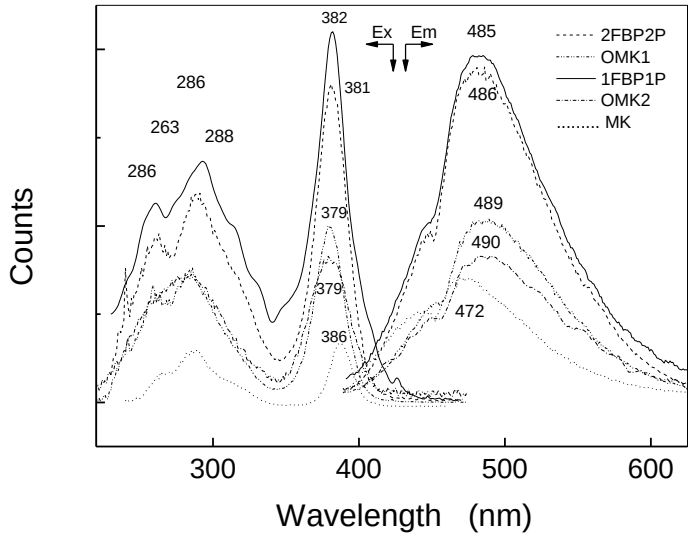

Fig. 3. The fluorescence spectra of PIs in CH_2Cl_2 ($c=1.47\times10^{-5}$M).

The maximum wavelength in the absorption spectrum for each compound was used in order to get its excitation spectrum. The emission signals with maximum peak (λ_{em}) at around 490 nm for OMKs were somewhat broadened and progressively red shifted with increasing molecular volume. The spectra of new PIs are reminiscent of that of MK. It means that the photochromophoric MK groups were conserved in the OMKs backbone under the polycondensation conditions. Compared with the 2FBP2P and 1FBP1P, the fluorescence intensity of OMKs was found to be lower. A possible reason for this is the inner-filter effect, which caused by local aggregation fluorophore, although the whole concentration is in a reasonable range according to the fluorescence behavior of MK. The Stokes shift decreases in the order OMK-2 (111nm)/OMK-1 (110nm) > 2FBP2P (105nm)/1FBP1P (103nm) > MK (86nm). This is indeed an unexpected result for macrophotoinitiators. In most cases, a smaller Stokes shift is observed when the fluorophore is immersed in the rigid and spatially restricted environment (e.g. in supramolecular system or under cryogenic conditions). This is apparently due to a smaller geometrical relaxation. However, in this system,

when the PI is excited to singlet state, energy can easily transfer along the soft aliphatic chain, which would favor the radiation less processes, leading to a less emissive species. This means that a restricted relaxation drops to negligibly small values (relative to the high efficient energy transfer). Finally, it leads to the increase of the Stokes shift. Likewise, energy transfer should result in a series of undistinguishable vibrational sub-levels of singlet state, which is responsible for the disappearance of mirror image.

As limited by the availability of the instruments, the result of phosphorescence spectra was not satisfied even if micellar-stabilized room-temperature phosphorescence was used.

Photochemistry and photopolymerization

Though for technical application the improvement of activity is of importance regardless of the mechanism, the understanding of the photolysis mechanism is crucial in view of the continuing effort to improve the efficiency of PIs in order to meet the requirements of new technologies. For example, an interesting point is whether the oligomeric PI will follow the same photolysis mechanism as the corresponding low molecular weight analog. In the ensuing discussion, we will take a closer look at the photochemical behavior of OMKs.

The UV spectra of OMK-2 under illumination with UV light are shown in Fig. 4. The main feature is the decrease of 345 nm band of OMK-2, and the increase at around 290 nm and 227 nm. There two new peaks may be assigned to the new photoproducts (e.g. Michler's pinacol or Michler's benzhydrol). Unfortunately, we cannot find out the UV/vis data of the above two compounds, while two similar compounds show the similar spectra (e.g. the values for N,N-dimethylaniline in the same solvent are λ_{max}=298nm/ε=2290 and 4,4'-bis(dimethylamino)diphenylmethane λ_{max} =303nm/ε=4830).

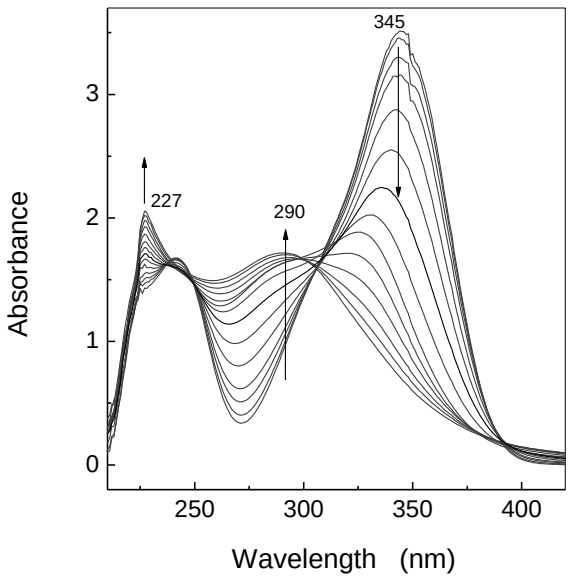

Fig. 4. The UV/vis spectra of OMK-2 in CH_2Cl_2 (1.3×10^{-4}M) as a function of the steady-state exposure time (0 s, 180 s, 300 s, then from 300 s to 2300 s with interval of 200 s).

Unlike MK, isoabsorptive point at 280 nm was not found in the UV/vis spectra, indicating that the photochemical reaction of OMKs proceeded with other concomitant reactions [12]. As we all know, at low concentration of MK, the photoreaction is essentially unimolecular reduction process [13]. At higher concentration, the photoreaction changes to bimolecular process and produces dimer [14]. Under our experimental conditions, unimolecular reduction seems to be the dominant process. However, taking a closer look at the macromolecular structure of PIs, one can conceive that heterogeneous system causes an increased concentration of MK fluorophore in the small region, and facilitating the bimolecular process. Consequently, this leads to the disappearance of the isoabsorptive point. While this is most likely the answer, we cannot exclude other assignments at this time.

It is well known that the photoreaction of Type II PIs proceeds via an electron-transfer/proton-transfer mechanism in the presence of hydrogen donors. It is clear that each of nitrogen atoms (N_a, N_b as marked in the Fig. 5) linked with three kinds of methylene group (–CH_2–N[CH_2–CH_2]$_2$N–Ar). Those H atoms of alpha methylene groups show a clear distinction according to the result of NMR. Since the key deprotonation of an alpha C–H bond is characteristic of tertiary amine, an interesting question is that which alpha methylene group mainly takes apart in the photoreaction when hydrogen transfer process takes place. To answer the question, we monitored the NMR signal of –CH_2– as a function of the steady-state UV exposure time. The result is shown in Fig. 6. It shows that, with the increase in irradiation time, the ^{1}H-NMR signal of H_c, H_d and H_e decreased, while that of H_f remains constant correspondingly. In particular, the H_d signal sharply decreases to a very low value. After prolonged irradiation, a new signal at 5.2 ppm was observed (indicated by the arrow, marked as H_x). The signal at 5.2 ppm is assigned to the *tert*-H of Michler's hydrol analog, $(CH_3)_2$N–Ar–<u>H</u>C(OH)–Ar–N$(CH_3)_2$. The appearance of Michler's hydrol analog is due to the reduction of MK ketyl radical. The continuous decrease of signals (H_c, H_d and H_e) reveals that all protons of alpha methylene group adjacent to N took part in the intramolecular/intermolecular H-abstraction reaction. This result indicates that hydrogen abstraction occurs partly at the carbon atom of (–CH_2–N[CH_2–C<u>H</u>$_2$]$_2$N–Ar–). This is easy to understand because hydrogen abstraction would lead to the formation of more stable benzylic radicals in this case. However deprotonation appears to be dominant with alpha C-H of aliphatic *tert*-amine (–CH_2–N[C<u>H</u>$_2$–CH_2]$_2$N–Ar–) and unimportant with that of aromatic *tert*-amine. The unexpected behavior of H_d can be explained in the following way: the photolysis reaction undergoes a primary process of electron transfer, followed by hydrogen atom abstraction process. In the former stages, two factors control the charge transfer process (1) basicity of N atom, as shown in Tab. 2, there is a general consensus that the basicity of aliphatic *tert*-amine is higher than aromatic *tert*-amine; (2) ionization energies (IE) of N atom. In the same table, the ionization energy of aliphatic *tert*-amine (e.g. triethylamine) is slightly higher than that of aromatic *tert*-amine analog (e.g. N,N-dimethylaniline). It seems that the eletctron transfer of aliphatic *tert*-amine (N_b) are less efficient than aromatic *tert*-amine according to IE. However, it is known that the efficiency of the deactivation of PI (e.g. thioxanthone) excited states is strongly related to the redox potential of the amine used. Electrochemical data show that triethylamine (TA, 0.76) is a stronger reducing agent than N,N-dimethylaniline (DA, 0.81) for its lower redox potentials (RP, $E_M^{+\bullet}{}_{/M}$), this leads to the conclusion contrary to that of IE. In the latter stages, the efficiency of hydrogen abstraction process can be influenced by bond dissociation energies (BDE)

of alpha C-H. Low BDE helps H_d to play an important role in the H transfer process. From the above reasoning, it is clear that deprotonation of alpha C-H (H_d) from aliphatic *tert*-amine (N_b) is the prevailed dominant photolysis mechanism of OMKs. The BDE, RP and basicity are the more important factors over IE in governing the transfer process at last.

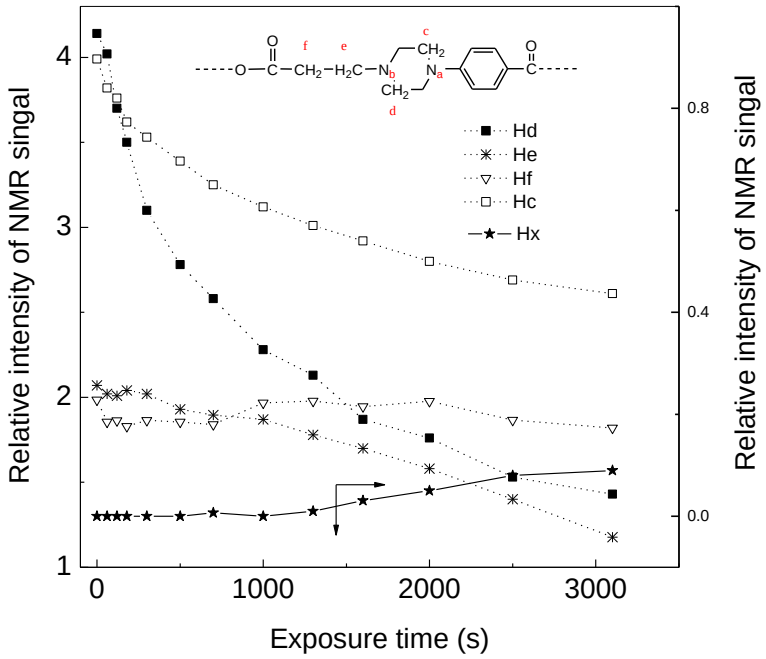

Fig. 5. Relative intensity of the NMR signals as a function of the steady-state UV exposure time for OMK-1 (1mol/L) in CH_2Cl_2. TMS was used as internal reference in terms of integrating area.

Tab. 2. Comparison of triethylamine (TA) and N,N-dimethylaniline(DA).

	pK_a* (25°C)	IE/$\Delta_f H_{ion}$ & (eV) /(kJ/mol)	RP ($E_M^{+\bullet}/M$)# (V)	BDE of α C-H & (kJ/mol)
TA	10.75	7.50±0.02 / 631	0.76	379.5
DA	5.07	7.12±0.02 / 787	0.81	383.7

#ref. [15], RP: redox potentials; &ref. [16]. IE: ionization energies; BED: bond dissociation energies

It is important to point out that, the H transfer never occurs between ester and carbonyl group. The study reported by R. M. Williams has shown that photoinduced intramolecular charge separation can be accomplished in systems in which donor and acceptor are spaced up to 15 Å by a saturated hydrocarbon bridge [17] . It is now commonly admitted that, most long-range charge/proton transfer are carried out under “extreme” conditions. An example of this behaviour can be found in DNA, where the π orbital along the stacking of base pairs facilitated the reaction [18].

Further insight into this photolysis mechanism could be attained by directly observing the changes UV spectra on irradiation of OMK in the presence of a small amount of TEMPO. Fig. 6 shows the influence of TEMPO on the UV spectra of OMK with the exposure time. TEMPO is known to be stable under our irradiation conditions. As a consequence, the formation of the photoproduct was strongly slowed down. It can be

quite simply explained that the carbon-centered radicals produced by H-abstraction was efficiently trapped by the nitroxyl radicals scavengers and quenched in the triplet state. From above studies, conclusions are drawn on the reaction mechanism of OMK. The proposed mechanism is shown in Fig. 7.

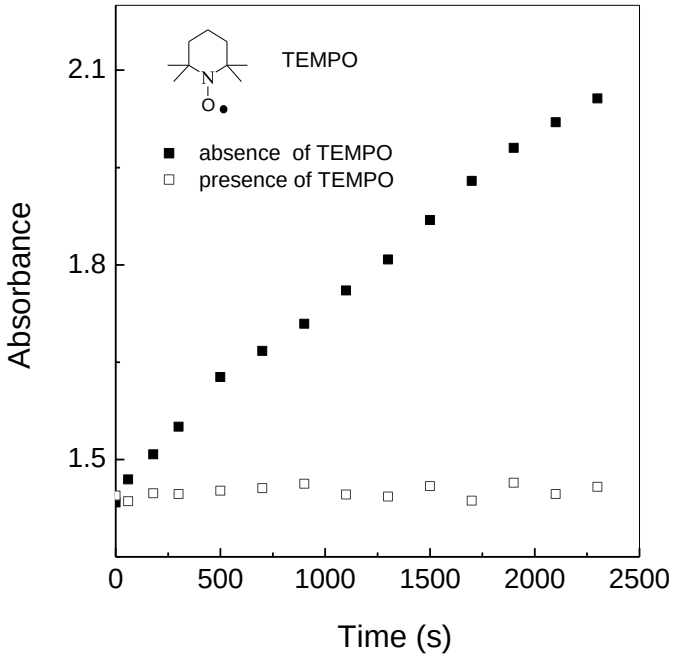

Fig. 6. UV-Vis spectra recorded during the photolysis of OMK-1 at 227 nm in CH_2Cl_2 (c_{TEMPO}= 2.7×10^{-5} mol.L^{-1}).

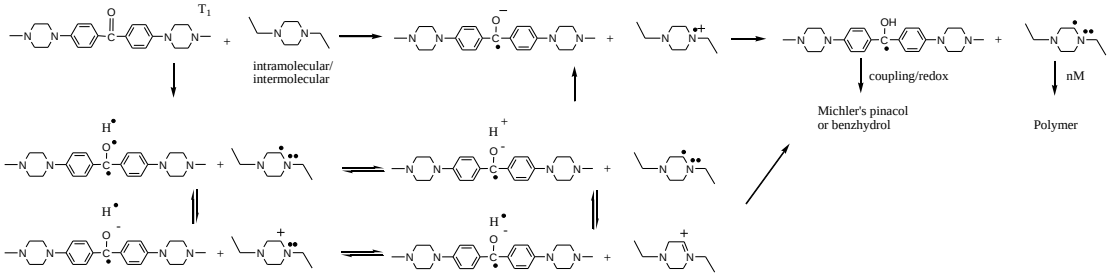

Fig. 7. Proposed mechanism for photolysis of the oligomeric OMK.

The photopolymerization of TMPTA initiated by several PIs were studied and the result are shown in Fig. 8. It showed that OMKs gave the highest polymerization rate whereas MK the lowest, but all the ultimate conversion was almost the same. This observation leads us to conclude that OMKs show better performance than MK based on a formulation of TMPTA. This behavior can be explained by three reasons: (1) More coinitiators (amine moiety) exist in an oligomer repeat unit, thus leading to a more efficient intramolecular/intermolecular H-abstraction reaction. (2) The aminoalkyl radicals were isolated by a long segment of acrylate residue groups, which results in reducing their tendency towards a radical recombination process. (3) Energy transfer along the polymer backbone may occur during irradiation, and thereby greatly enhance the photoactivity. Y. Yagci and S. Jockusch, et al believed that the higher activity of the hybrid PI is mainly due to the double functionality of the

initiator. Triplet PI reacts with ground state PI by hydrogen abstraction to produce PI•, which initiate the polymerization and incorporate into the polymer (PI-polymer). PI-polymer can be photo-excited again during the course of the polymerization to generate triplet PI-polymer, which can abstract hydrogen from PI to produce the initiating PI•. This possibility does not exist for the two-component system [19], where PI and coinitiator are separate from each other.

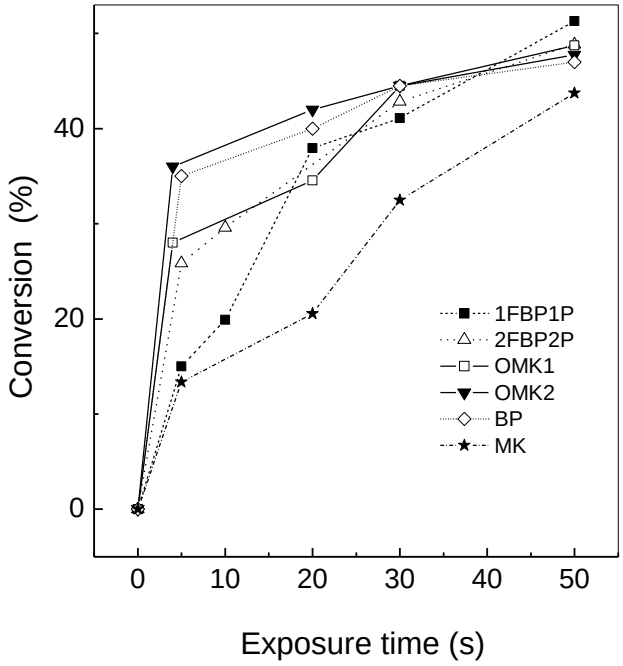

Fig. 8. Conversion curves for TMPTA initiated by 4.0wt% MK, 4.0wt % 1FBP1P, 5.2wt % 2FBP2P, 8.8 wt% OMK-1 and 9.8 wt% OMK-2 (by equal molar conc. of carbonyl group), room temperature, air atmosphere, light intensity: 1.5 mW·cm^{-2}

OMKs were found to be slightly higher effective than the corresponding small molecular analog (2FBP2P and 2FBP2P). Although aliphatic NH transfers H efficiently to triplet carbonyl chromophore, the ketyl and aliphatic alkylaminyl (N-centered) radicals largely react to regenerate starting materials, as had been validated by low quantum yield of reductions of BP by primary and secondary amines [20]. It is one of the possible reason that aliphatic tertiary amine as a co-initiator appears to be more popular than secondary amine in the formulation of UV-curing.

Volatility and migration

PIs which are not totally consumed during the curing process, especially in the deep layer of coating, may volatilize to the atmosphere during room temperature storage. We simulate the situation of the food saved in the package in order to evaluate the volatile behavior of PIs in the Torrid Zone or in summer, in particular volatile aldehydic derivatives. The results are shown in Fig. 9. It can be seen that after storage for 10 h at 60 °C, all PIs were practically not released, while weight loses about 100% and 20% were found for TEA and BP. Both of them show high vapor pressure (0.0019 mm Hg at 25 °C for BP and 0.01 mm Hg at 20 °C for TEA) because of low melting point (48 °C for BP and 18 °C for TEA) [21] . So far as it goes, very low volatility can be expected for PIs except BP when applied to UV curing formulation.

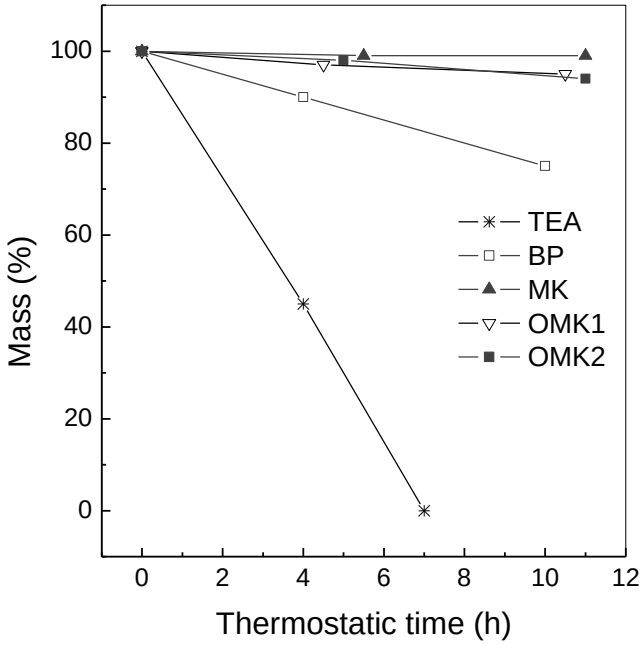

Fig. 9. Plot of residual mass of PIs *vs.* time at constant temperature (60 °C in air atmosphere).

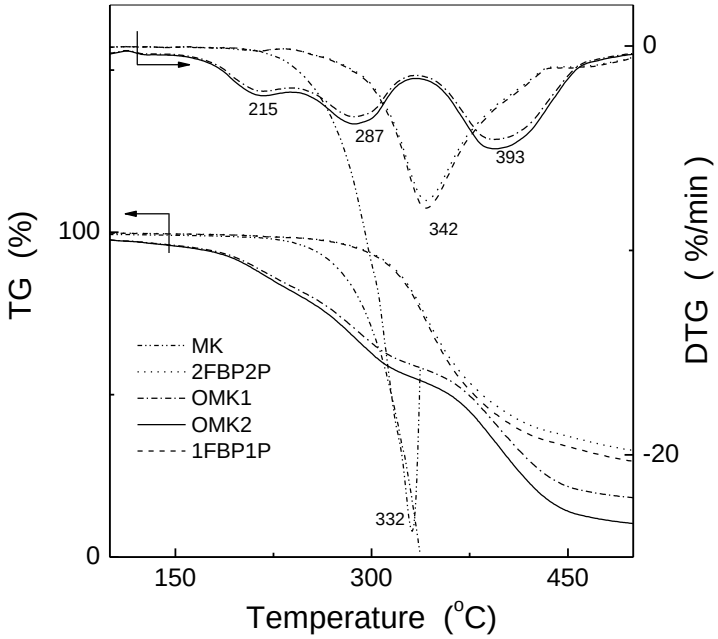

Fig. 10. TG and DTG curves for three PIs in N_2, heating rate: 10 °C /min.

In order to evaluate the thermolysis limit of application, we have therefore used TG to elucidate thermal decomposition of PIs and the results are shown in Fig. 11. The weight-loss for OMKs, started at 150 °C and completed at 450 °C with a mass loss of about 80%, is considered to be mainly due to the thermal decomposition. The main weight-loss temperature located at 215, 287 and 393 °C, as is indicated by the DTG

curve. The former two weight-loss maybe tentatively assigned to thermal decomposition of ester and ether group, and the last weight-loss at 393 °C was readily assigned to MK moiety according to the TG result of the corresponding low molecular weight analog (MK, 1FBP1P and 2FBP2P). The excellent thermal stability of OMKs mean less volatility, which is beneficial to the olfaction aesthetic effect while used as PI in UV-curable coatings and inks for the decoration of goods package.

The migration test focused on simulating oily foods that may have been exposed to or contacted with PIs as chemical migrants from either primary or secondary printed packaging. The BP measured in our test ranged from 25.1 mg/kg to 4.5 mg/kg, with an average level of 10.3 mg/kg. The average of MK obtained here is on the same order as BP but higher (detection in terms of BP chromophore). These values are significantly higher than the specific legislation for food contact plastics by Group Tolerable Daily Intake (TDI), Directive 2002/72/EC (for BP is 0.6 mg/kg, bodyweight) [22]. On the contrary, no migration of OMKs from extract lacquers is observed. This was attributed in part to the fact that the oligomer has several active centers within a repeat unit, which may lead to the existence of biradical/multiradical intermediates in the photochemical outgrowth. This increases the initiating efficiency or the probability of a fragment bonded to the backbone of the formed polymer chain, thus obtaining the properties of low migration. Under the conservative considerations, OMKs are suitable for use in formulations when the health effects must be taken into account.

In additional investigation, it has been found that the solid PIs were readily soluble in various acrylate monomers. Besides, the yellowing of coatings is very similar with 4,4’-bis(diethylamino)benzophenone(DEAB). The result obtained by GPC indicates that the average polymerization degree of OMKs was only about 2 or 3 in a molecule. Considering material compatibility, we prefer oligomer to macromolecule. Limited by the length of this article, the toxicological testing will be discussed in a forthcoming article.

Conclusions

In conclusion, OMKs are efficient oligomeric PIs for free radical polymerization. It does not require an additional hydrogen donor since the hydrogen donating groups is incorporated into chain ends/side chains. In addition, it possesses excellent optical absorption properties in the near UV spectral region, ensuring efficient light absorption from most UV-curing tools. They can be used to initiate acrylate polymerization with a higher efficiency. They do not release any odor nor show any migration in the reported conditions. These properties suggest that it may find use in green manufacturing industry.

Experimental

Materials

4,4’-Difluorobenzophenone,4-fluorobenzophenone and piperazine were obtained from Aldrich. The monomers, such as 1,6-hexanediol diacrylate (HDDA), trimethylolpropane triacrylate (TMPTA), 2-hydroxyethyl methacrylate (HEMA), triethyleneglycol diacrylate (TEGDA) were provided by Cognis. BP and MK were chosen as PIs for comparison and purchased from Ciba. MK and BP for spectral analysis were purified.

Methods

-Spectroscopy

UV/vis absorption spectra were obtained with a Varian Cary100 spectrometer using dichloromethane as solvent. Fluorescence spectra were obtained with a FLS920 spectrometer (Edinburgh Instruments Corp.). FT-IR spectra were obtained with a Thermo Nicolet Nexus^{TM} 670 FT-IR E.S.P. spectrometer (USA). NMR spectra were obtained on a Varian Mercury 300M (Palo Alto, CA) spectrometer using $CDCl_3$ as solvent. In the photochemical section, the samples for NMR were dissolved in redistilled CH_2Cl_2 and sealed in a small capillary, which was placed in an NMR tube filled with $CDCl_3$ at ambient temperature. For non-resolved NMR peaks, Lorentzian analysis of Origin software was used to separate peak to obtained reasonably reproducible results and low error of NMR integral area.

-GPC

The number average molecular weight (M_n) and weight average molecular weight (M_w) of the oligomers were measured by GPC (Breeze GPC, Waters Corp.) using THF as solvent.

-TG

Thermogravimetric analysis (TGA; TG-209C, Netzsch Corp.) was carried out from room temperature to 600 °C at a heating rate of 10 °C/min under a nitrogen atmosphere. Constant temperature TGA was carried out in a thermostatic oven (100 °C) for 10 h under a nitrogen atmosphere.

Photoinitiating activity

The light intensity was measured by a UV-radiometer (type UV-A, Photoeletric Instrument Factory, Beijing Normal University, China), which is sensitive in the wavelength range of 320-400 nm. The samples containing 1-5 wt% of the initiator was sonicated for 15 min to ensure complete dissolving. The IR technique was employed to evaluate the photoinitiating efficiency of new PIs in comparison with MK as described in the literature [23]. The =C-H out of plane bending at 812cm^{-1} was used to monitor acrylate polymerization. The effect of thickness in the systems was eliminated by the use of peak area of ester groups at 1730cm^{-1} as an internal standard. Conversion was calculated using the following Eq.

$$Conversion = \frac{A_0\text{-}A_t}{A_0} \times 100\% \quad (1)$$

where A_0 is the corrected peak area before irradiation and A_t is the corrected peak area at time *t*.

Migration test

UV-curing films were prepared from HDDA irradiated by a PI under the same experimental conditions. Eight films with the same thickness and area were extracted with the same amount of ethanol containing 0.4 per cent triethylamine. The detective amount of PIs extracted from films was determined by fluorimetry. Blank tests were carried out without samples. BP chromophore of all PIs was used as standard for

calculation. The extract of BP was analyzed by GC-MS as described in the literature [24].

Synthesis of oligomeric PI

The synthetic route is shown in Fig. 2.

-Nucleophilic substitition reaction

2FBP2P: 0.03mol of 4,4'-difluorobenzophenone, 0.1mol of anhydrous piperazine, 0.1 mol of potassium carbonate and 300 mL of DMSO were mixed together. The reaction mixture was stirred at 90 °C for 20 h and subsequently poured into the mixture of hydrochloric acid and ice, then was treated with dilute sodium hydroxide solution to the basic. The product was extracted with dichloromethane, and dried over anhydrous sodium sulfate. The solvent was then removed using a vacuum evaporator. The residue was poured into ethyl ether to give precipitated product of 2FBP2P with yield of 95%, m.p. 171 °C. FT-IR (KBr pellet, cm^{-1}): 3424 (ν N-H), 3071(ν aromatic C-H), 2831 (ν CH_2, CH_3), 1628 (ν C=O), 1598 (ν aromatic C=C); ^{1}H NMR (300MHz, $CDCl_3$, δ ppm): 1.60 (s, 2H, N-H), 3.04 (t, 8H, J=9Hz, CH_2-NH), 3.32 (t, 8H, J=9Hz, N-CH_2-CH_2), 6.90 (d, 4H, J=9.0Hz, aromatic CH close to N atom), 7.74 (d, 4H, J=9.0Hz, aromatic CH close to carbonyl group); ^{13}C NMR (300MHz, $CDCl_3$, δ ppm): 46.2 (CH_2-NH-), 49.2 (N-CH_2-CH_2), 113.7 (aromatic CH close to N atom), 128.6 (aromatic C adjacent to C=O group), 132.1 (aromatic CH close to C=O group), 154.1 (aromatic C adjacent to N atom), 203.0 (C=O); FAB-MS: cacl. M=350 for $C_{21}H_{26}N_4O$ and found $(M+1)^+$ =351; Elem. Anal. Calcd. for $C_{21}H_{26}N_4O$: C 71.97%, H 7.48%, N 15.99%. Found: C 69.63%, H 7.25%, N 14.90%.

1FBP1P: 0.06 mol of 4-fluorobenzophenone, 0.1mol of anhydrous piperazine and other steps were the same as the above procedure. Yield of 98%, m.p. 165 °C. FT-IR (KBr pellet, cm^{-1}): 3420(ν N-H), 3075(ν aromatic C-H), 2812 (ν CH_2, CH_3), 1630(ν C=O), 1605 (ν aromatic C=C); ^{1}H NMR (300MHz, $CDCl_3$, δ ppm): 1.60 (s, 1H, N-H), 3.04 (t, 4H, J=9Hz, CH_2-NH), 3.34 (t, 4H, J=9Hz, N-CH_2-CH_2), 6.90 (d, 2H, J=9.0Hz, aromatic CH close to N atom), 7.44 (t, 2H, J=9.0Hz, aromatic *m*-CH), 7.53 (t, 1H, J=9.0Hz, aromatic *p*-CH); 7.70 (d, 2H, J=9.0Hz, aromatic *o*-CH), 7.79 (d, 2H, J=9.0Hz, aromatic CH close to carbonyl group); ^{13}C NMR (300MHz, $CDCl_3$, δ ppm): 46.0 (CH_2-NH-), 48.6 (*tert*-N-CH_2-CH_2), 113.6 (aromatic CH close to N atom), 127.5 (aromatic C adjacent to C=O group), 128.3 (aromatic *m*-CH), 129.7 (aromatic *o*-CH), 131.6 (aromatic CH close to C=O group), 132.7 (aromatic *p*-CH), 139.0 (aromatic C adjacent to C=O group) 154.4 (aromatic C adjacent to N atom), 195.3 (C=O); FAB-MS: cacl. M=266 for $C_{17}H_{18}N_2O$ and found $(M+1)^+$ =267; Elem. Anal. Calcd. for $C_{17}H_{18}N_2O$: C 76.66%, H 6.81%, N 10.52%. Found: C 76.12%, H 6.82%, N 10.70%.

-Michael addition

OMK-2: 0.07 mol of 2FBP2P, 0.07mol of TEGDA, a small amount of catalyst DBU and 300 mL of methanol were mixed together. The reaction lasted for 7 h at 40-50 °C. The reaction mixture was filtrated. Methanol was then removed using a vacuum evaporator. The residue was poured into ethyl ether to yield viscous liquid product. The product was separated out and dried in a vacuum oven. Yield was 75~80%. The crude product was dissolved in dichloromethane, then concentrated using a vacuum evaporator, and then poured into ethyl ether to yield fine product. FT-IR (KBr pellet, cm^{-1}): 3408(ν N-H), 2944(ν aromatic C-H), 2851 (ν CH_2, CH_3), 1729 (ν COO), 1634

(ν C=C), 1628 (ν C=O), 1596 (ν aromatic C=C), 1223(ν C-O- C), 810 (δ C=C); GPC: M_n=2160(max.).

a:

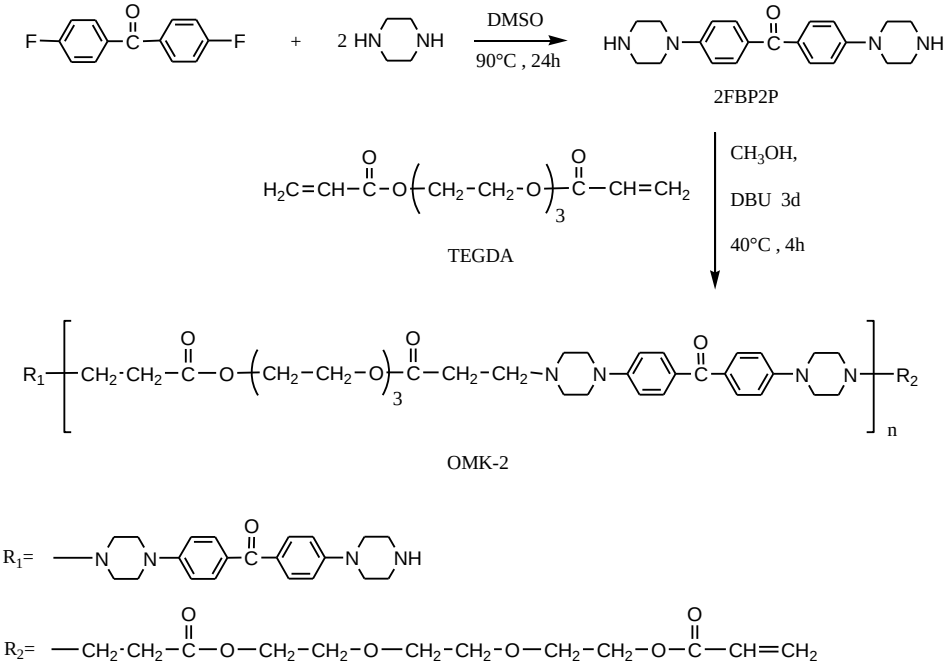

b:

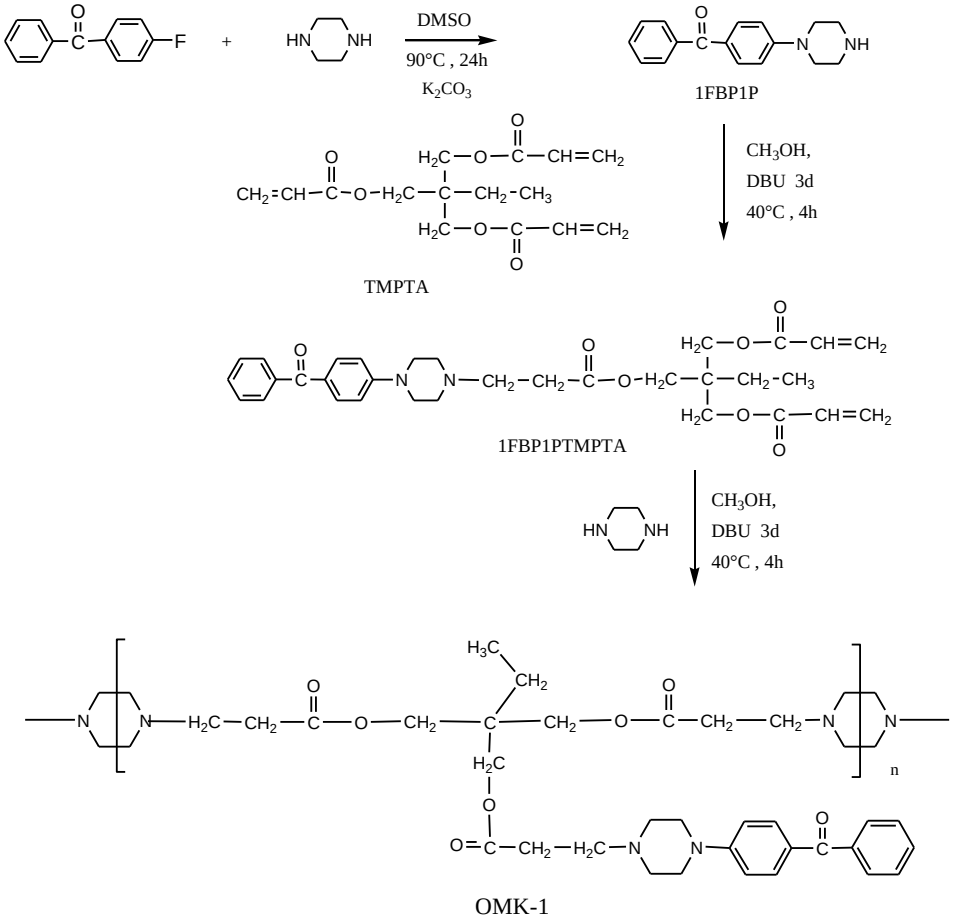

Fig. 11. Synthetic route of oligo(Michler's Ketone) (a:OMK-2 ; b:OMK-1).

OMK-1: 0.05mol of 1FBP1P and 0.2mol of TMPTA undergo Michael addition to produce 1FBP1PTMPTA following the above procedure. The product was dissolved in dichloromethane, and the concentrated solution was poured into petroleum ether. Precipitate was dried in a vacuum oven. FT-IR (KBr pellet, cm^{-1}): 2944(ν aromatic C-H), 2851 (ν CH_2, CH_3), 1729 (ν COO), 1634 (ν C=C), 1628 (ν C=O), 1596 (ν aromatic C=C), 810 (δ C=C); ^{1}H NMR (300MHz, $CDCl_3$, δ ppm): 0.92 (m, 3H, J=?Hz, $C\underline{H}_3$-CH_2-), 1.27(m, 2H, J=?Hz, CH_3-$C\underline{H}_2$-), 2.62 (m, 4H, CH_2-N-$C\underline{H}_2$-CH_2-COO), 2.69 (m, 8H, Ar-N-CH_2-$C\underline{H}_2$-), 2.82 (t, 4H, CH_2-N-CH_2-$C\underline{H}_2$-COO), 3.39 (t, 8H, Ar-N-$C\underline{H}_2$), 5.80 (d, 1H, -CH=CH-$\underline{H}$(*trans*)), 6.09 (m, 1H, -$C\underline{H}$=CH_2), 6.36 (d, 1H, CH=CH-$\underline{H}$(*cis*)), 6.90 (d, 2H, J=9.0Hz, aromatic $C\underline{H}$ close to N atom), 7.44 (t, 2H, J=9.0Hz, aromatic *m*-$C\underline{H}$), 7.53 (t, 1H, J=9.0Hz, aromatic *p*-$C\underline{H}$); 7.70 (d, 2H, J=9.0Hz, aromatic *o*-$C\underline{H}$), 7.79 (d, 2H, J=9.0Hz, aromatic $C\underline{H}$ close to carbonyl group); ^{13}C NMR (300MHz, $CDCl_3$, δ ppm): 8.5($\underline{C}H_3$-), 23.4(CH_3-$\underline{C}H_2$), 32.2(Ar-N-CH_2-$\underline{C}H_2$-N), 48.6 (Ar-N-$\underline{C}H_2$-CH_2), 52.8(N-CH_2-$\underline{C}H_2$-COO), 53.6 (N-$\underline{C}H_2$-CH_2-COO), 64.4(N-CH_2-CH_2-COO-$\underline{C}H_2$-), 113.6 (aromatic $\underline{C}$H close to N atom), 127.5 (aromatic $\underline{C}$ adjacent to C=O group), 128.3($\underline{C}H_2$=CH-), 128.3 (aromatic *m*-$\underline{C}$H), 129.7 (aromatic *o*-$\underline{C}$H), 130.8(CH_2=$\underline{C}$H-), 131.6 (aromatic $\underline{C}$H close to C=O group), 132.7 (aromatic *p*-$\underline{C}$H), 139.0 (aromatic $\underline{C}$ adjacent to C=O group), 154.4 (aromatic $\underline{C}$ adjacent to N atom), 172.6 ($\underline{C}$OO-), 195.3 ($\underline{C}$=O). GPC: M_n<1000.

OMK-1 was obtained by further addition of a 1:1 stoichiometric ratio of 1FBP1PTMPTA and piperazine under the same condition as the aforementioned experiment. GPC: M_n=3260(max.). Total synthetic process is shown in Fig. 11.

Acknowledgements

This work was supported by the National Natural Science Foundation of China(NSFC), Grant No. 20874022 .

References

[1] Duz, B.; Onen, A.; Yagcı, Y. and *Die Angewandte Makromolekulare Chemie* **1998**, 2581(1-4), 4462.
[2] Sundararajan, C. "*N-methyl-4-picolinium esters as photoremovable protecting groups based on photoinduced electron transfer*", PhD Thesis, University of Maryland, **2005**.
[3] Angiolini, L.; Caretti, D.; Carlini, C.; Corelli, E.; Fouassier, J.P.; Morlet-Savary, F.; *Polymer*, **1995**, 36(21), 4055.
[4] Ghosh, N.N.; Kiskan, B.; Yagci, Y. *Prog. Polym. Sci.* **2007**, 32,1344.
[5] Liska, R. *J. Polym. Sci. A: Polym. Chem.* **2004**, 42(9), 2285.
[6] Koch, T.H.; Jones, A.H.; *J. Am. Chem. Soc.* 1970, *92*,7503.
[7] Yang, J.W.; Zeng, Z.H.; Chen, Y.L.; *J. Polym. Sci. A: Polym. Chem.* **1998**, *36(14)*, 2563.
[8] Ye, G.D.; Yang, J.W.; Zeng, Z.H. and Chen, Y.L. *J. Appl. Polym. Sci.* **2006**, *99*, 3417.
[9] Ye, G.D.; Ke, Z.F.; Yang, J.W.; Zhao, T.Y.; Zeng, Z.H. and Chen, Y.L. *Polymer.* **2006**, *47*, 4603.
[10] Spange, S.; Keutel, D. *Ann. Chem.* **1992**, 423.
[11] Urahata, S.; Canuto, S. *Int. J. Quant. Chem.* **2000**, *80*, 1062.
[12] Sarker, A.M.; Sawabe, K.; Neckers, D.C. *Macromolecules* **1999**, *32(16)*, 5203.
[13] Koch, T.H.; Jones, A.H. *J. Am. Chem. Soc.* **1973**, *95(3)*, 986.
[14] Suppan, P. *J. Chem. Sci., Fara. Trans. 1.* **1975**, *71*, 539.

[15] Wurpel, G.W.H.; "*Photoinduced Dynamics in Hydrogen-Bonded Rotaxanes*", PhD Thesis, University of Amsterdam, **2001**, Jun.
[16] Luo, Y.R. *Handbook of bond dissociation energies in organic compounds,* London: CRC Press LLC **2003**, 84.
[17] Williams, R. M.; "*Fullerenes as Electron Accepting Components in Supramolecular and Covalently Linked Electron Transfer Systems*". PhD Thesis, University of Amsterdam, **1996**. Jun.
[18] Chang, Ch.M.; Neto, A.H.C. and Bishop, A.R. *Chem. Phys.* **2004**, *303(1-2):2*, 189.
[19] Cokbaglan, L.; Arsu, N.; Yagci, Y.; Jockusch, S. and Turro, N.J.; *Macromolecules* **2003**, *36*, 2649.
[20] Inbar, S.; Linschitz, H. and Cohen, S.G. *J. Am. Chem. Soc.* **1981**, *103*, 1048.
[21] Thomas, S.WIII; Amara, J.P.; Bjork, R.E. and Swager, T.M. *Chem. Commun.* **2005**, *36*, 4572.
[22] UK Food Standards Agency; *Food Survey Information Sheet* **2006**,*18(06)*, 1.
[23] Lee, T.Y.; Roper, T.M.; Kudyakov, I.; Viswanathan, K.; et al. *Polymer.* **2003**, *44*, 2859.
[24] Johns, S.M.; Jickells, S.M.; Read, W.A.; Castle, L. *Packag. Technol. Sci.* **2000**,*13*, 99.